J. Plasma Phys. (2024), *vol*. 90, 905900105
Published by Cambridge University Press

doi:10.1017/S0022377823001356

The gap-size influence on the excitation of magnetorotational instability in cylindricTaylor–Couette flows

G. Rüdiger [1,2,†] **and M. Schultz**[2]

[1]Institute of Physics and Astronomy, University of Potsdam, Karl-Liebknecht-Str. 24-25, 14476 Potsdam, Germany

[2]Leibniz-Institut für Astrophysik Potsdam, An der Sternwarte 16, D-14482 Potsdam, Germany

(Received 14 April 2023; revised 25 November 2023; accepted 27 November 2023)

The excitation conditions of the magnetorotational instability (MRI) are studied for axially unbounded Taylor–Couette (TC) flows of various gap widths between the cylinders. The cylinders are considered as made from both perfect-conducting or insulating material and the conducting fluid with a finite but small magnetic Prandtl number rotates with a quasi-Keplerian velocity profile. The solutions are optimized with respect to the wavenumber and the Reynolds number of the rotation of the inner cylinder. For the axisymmetric modes, we find the critical Lundquist number of the applied axial magnetic field: the lower, the wider the gap between the cylinders. A similar result is obtained for the induced cell structure: the wider the gap, the more spherical the cells are. The marginal rotation rate of the inner cylinder – for a fixed size of the outer cylinder – always possesses a minimum for not too wide and not too narrow gap widths. For perfect-conducting walls the minimum lies at $r_{\rm in} \simeq 0.4$, where $r_{\rm in}$ is the ratio of the radii of the two rotating cylinders. The lowest magnetic field amplitudes to excite the instability are required for TC flows between perfect-conducting cylinders with gaps corresponding to $r_{\rm in} \simeq 0.2$. For even wider and also for very thin gaps the needed magnetic fields and rotation frequencies are shown to become rather huge. Also the non-axisymmetric modes with $|m| = 1$ have been considered. Their excitation generally requires stronger magnetic fields and higher magnetic Reynolds numbers in comparison with those for the axisymmetric modes. If TC experiments with too slow rotation for the applied magnetic fields yield unstable modes of any azimuthal symmetry, such as the currently reported Princeton experiment (Wang *et al.*, *Phys. Rev. Lett.*, vol. 129, 115001), then also other players, including axial boundary effects, than the MRI-typical linear combination of current-free fields and differential rotation should be in the game.

Keywords: astrophysical plasmas, plasma instabilities, plasma flows

† Email address for correspondence: gruediger@aip.de

1. Introduction and motivation

Taylor–Couette (TC) flows with conducting fluids between two rotating cylinders are favorable for an experimental realization of the various versions of the magnetorotational instability (MRI) for which the applied magnetic field is always current-free (Velikhov 1959; Ji, Goodman & Kageyama 2001; Rüdiger & Zhang 2001; Schartman, Ji & Burin 2009; Schartman *et al.* 2012). If the field is spiral rather than axial, the necessary Reynolds numbers and Hartmann numbers are surprisingly small (Hollerbach & Rüdiger 2005; Rüdiger *et al.* 2006) which made it possible to investigate the corresponding helical version of MRI (HMRI) with the Promise experiment (Stefani *et al.* 2006). The resulting instability modes are axisymmetric and they are migrating along the rotation axis. The closely related azimuthal MRI (AMRI) appears when working with current-free toroidal fields for which the unstable modes are non-axisymmetric (Ogilvie & Pringle 1996; Hollerbach, Teeluck & Rüdiger 2010; Seilmayer *et al.* 2014).

The mentioned experiments have used one and the same container construction where the inner radius was 50 % of the outer radius, i.e. $r_{\rm in} = R_{\rm in}/R_{\rm out} = 0.5$. For this geometry the rotation law $\Omega \propto R^{-q}$ leads to a shear $\mu = \Omega_{\rm out}/\Omega_{\rm in}$ for quasi-Keplerian rotation with $q = 1.5$ of $\mu = 0.35$. In a recent paper the Princeton group presented experimental results related to the standard version of MRI (SMRI), with a purely axial field being applied, using a container with $r_{\rm in} = 0.35$ and the aspect ratio $\Gamma = H/(R_{\rm out} - R_{\rm in}) = 2.1$. The flow between the cylinders is described by $\mu = 0.19$, while the quasi-Keplerian flow in such a container is defined by $\mu = 0.21$ (Wang *et al.* 2022*b*).

After our previous numerical results for $r_{\rm in} = 0.5$, for very small magnetic Prandtl number and for perfectly conducting walls, the absolute minimum of the magnetic Reynolds number for the excitation of marginal instability was 21.3 for a shear flow with $\mu = 0.33$, which is somewhat steeper than the Keplerian rotation law with $\mu = 0.35$ (Rüdiger *et al.* 2018*a*). Both of these slightly super-Keplerian rotation laws follow $\mu = r_{\rm in}^q$ with $q = 1.59$.

The model of a homogeneous fluid contained between two vertically unbounded rotating cylinders is used with a uniform magnetic field parallel to the rotation axis. For viscous flows the general form of the rotation law $\Omega(R)$ of the fluid is

$$\Omega(R) = a + \frac{b}{R^2}, \tag{1.1}$$

where a and b are the two constants related to the angular velocities $\Omega_{\rm in}$ and $\Omega_{\rm out}$, with which the inner and the outer cylinders are rotating, and R is the distance from the rotation axis. If $R_{\rm in}$ and $R_{\rm out}$ ($R_{\rm out} > R_{\rm in}$) are the radii of the two cylinders, then

$$a = \frac{\mu - {r_{\rm in}}^2}{1 - {r_{\rm in}}^2}\Omega_{\rm in} \quad \text{and} \quad b = R_{\rm in}^2 \frac{1-\mu}{1-{r_{\rm in}}^2}\Omega_{\rm in}, \tag{1.2a,b}$$

with the above defined geometry parameters μ and $r_{\rm in}$. Following the Rayleigh stability criterion,

$$\frac{{\rm d}(R^2\Omega)^2}{{\rm d}R} > 0, \tag{1.3}$$

rotation laws are hydrodynamically stable for $a > 0$, i.e. $\mu > r_{\rm in}^2$. They should in particular be stable for a resting inner cylinder, i.e. $\mu \to \infty$ (superrotation).

The present paper has two motivations. The first one concerns the question of the dependence of the eigenvalues on the gap width of the container. The ratio $r_{\rm in}$ of the two-cylinder radii is the only free parameter describing the geometry of the axially

https://doi.org/10.1017/S0022377823001356 Published online by Cambridge University Press

unbounded container. It is so far unknown how the gap width determines the critical rotation rate for a given magnetic field, and also the wavenumber of the excited instability pattern. The latter result will have consequences for necessary vertical extension of a possible experimental set-up.

We work with the magnetic Prandtl number

$$Pm = \frac{\nu}{\eta}, \tag{1.4}$$

with ν being the kinematic viscosity and η the magnetic diffusivity. The equations are solved for the very small magnetic Prandtl number $Pm = 10^{-5}$ close to the value for liquid sodium. For small magnetic Prandtl numbers the excitation conditions for the standard magnetorotational instability only depend on the microscopic magnetic diffusivity rather than the molecular viscosity, so that even Pm does not play a role (Rüdiger & Shalybkov 2002). The ratio of the container wall radii is varied from $r_{\rm in} = 0.1$ to $r_{\rm in} = 0.9$. We shall see that between these values the critical magnetic Reynolds number of rotation possesses a minimum while the critical Lundquist number of the applied magnetic field linearly grows with $r_{\rm in}$.

Our second question is the difference of the excitation conditions for axisymmetric and non-axisymmetric modes. Though it is widely known that the mode with the easiest excitation is the axisymmetric one, it is still important to know how much more difficult the excitation of a non-axisymmetric mode is.

2. Basic equations

The magnetohydrodynamics equations which have to be solved are

$$\frac{\partial \boldsymbol{u}}{\partial t} + (\boldsymbol{u}\nabla)\boldsymbol{u} = -\frac{1}{\rho}\nabla p + \nu\Delta\boldsymbol{u} + \frac{1}{\rho}\boldsymbol{J}\times\boldsymbol{B} \tag{2.1}$$

and

$$\frac{\partial \boldsymbol{B}}{\partial t} = \nabla\times(\boldsymbol{u}\times\boldsymbol{B}) + \eta\Delta\boldsymbol{B}, \tag{2.2}$$

with the electric current

$$\boldsymbol{J} = \frac{1}{\mu_0}\nabla\times\boldsymbol{B} \tag{2.3}$$

and with $\nabla\boldsymbol{u} = \nabla\boldsymbol{B} = 0$. They must be considered in a cylindrical geometry with R, ϕ and z as the coordinates. A viscous electric-conducting incompressible fluid between two rotating infinite cylinders in the presence of a uniform magnetic field parallel to the rotation axis leads to the basic solution $U_R = U_z = B_R = B_\phi = 0, B_z = B_0 =$ const. and $U_\phi = aR + b/R$, with $\boldsymbol{U}$ as the flow and $\boldsymbol{B}$ as the magnetic field. We are interested in the stability of this solution. The perturbed state of the flow may be described by $u'_R,\ u'_\phi,\ u'_z,\ p', B'_R,\ B'_\phi,\ B'_z$ with p' as the pressure perturbation.

In the following only the linear stability problem will be considered. By expansion of the disturbances into normal modes the solutions of the linearized equations are of the form

$$\boldsymbol{u}' = \boldsymbol{u}(R)\exp(\mathrm{i}(m\phi + kz + \omega t)), \quad \boldsymbol{B}' = \boldsymbol{B}(R)\exp(\mathrm{i}(m\phi + kz + \omega t)). \tag{2.4a,b}$$

From here on all dashes are being omitted from the symbols of fluctuating quantities. The marginal stability line is defined where the imaginary part $\mathrm{Im}(\omega)$ vanishes. We shall

https://doi.org/10.1017/S0022377823001356 Published online by Cambridge University Press

always use the geometrical average

$$R_0 = \sqrt{(R_{\rm out} - R_{\rm in})R_{\rm in}} \tag{2.5}$$

as the unit of length, η/R_0 as the unit of velocity and B_0 as the unit of the magnetic field. We note the rather weak dependence of R_0 on the value of $r_{\rm in}$ as long as $0.2 \le r_{\rm in} \le 0.8$. The R_0 only becomes small for $r_{\rm in} \to 0$ or for $r_{\rm in} \to 1$, i.e. for very wide or for very narrow gaps between the cylinders. Its maximum $R_0 = 0.5R_{\rm out}$ is reached for $r_{\rm in} = 0.5$. In order to denormalize quantities, R_0^{-1} is used as the unit of wavenumbers and ν/R_0^2 as the unit of frequencies.

Using the same symbols for normalized quantities, the equations can be written as a system of 10 equations of first order, i.e.

$$\frac{{\rm d}u_R}{{\rm d}R} = -\frac{u_R}{R} - {\rm i}\frac{m}{R}u_\phi - {\rm i}ku_z, \tag{2.6}$$

$$\frac{{\rm d}u_\phi}{{\rm d}R} = X_2 - \frac{u_\phi}{R}, \quad \frac{{\rm d}u_z}{{\rm d}R} = X_3, \tag{2.7a,b}$$

$$\begin{aligned}\frac{{\rm d}X_1}{{\rm d}R} &= \left(\frac{m^2}{R^2} + k^2\right)u_R + {\rm i}(\omega + mRe\,\Omega)u_R \\ &\quad + 2{\rm i}\frac{m}{R^2}u_\phi - 2Re\,\Omega u_\phi - {\rm i}kHa^2B_R,\end{aligned} \tag{2.8}$$

$$\begin{aligned}\frac{{\rm d}X_2}{{\rm d}R} &= \left(\frac{m^2}{R^2} + k^2\right)u_\phi + {\rm i}(\omega + mRe\,\Omega)u_\phi \\ &\quad - 2{\rm i}\frac{m}{R^2}u_R + 2aRe\,u_R - {\rm i}kHa^2B_\phi \\ &\quad + \frac{m^2}{R^2}u_\phi + k\frac{m}{R}u_z - {\rm i}\frac{m}{R}X_1,\end{aligned} \tag{2.9}$$

$$\begin{aligned}\frac{{\rm d}X_3}{{\rm d}R} &= \left(\frac{m^2}{R^2} + k^2\right)u_z + {\rm i}(\omega + mRe\,\Omega)u_z \\ &\quad - \frac{X_3}{R} - {\rm i}kHa^2B_z + k\frac{m}{R}u_\phi + k^2u_z - {\rm i}kX_1,\end{aligned} \tag{2.10}$$

$$\frac{{\rm d}B_R}{{\rm d}R} = -\frac{B_R}{R} - {\rm i}\frac{m}{R}B_\phi - {\rm i}kB_z, \quad \frac{{\rm d}B_\phi}{{\rm d}R} = X_4 - \frac{B_\phi}{R}, \tag{2.11a,b}$$

$$\frac{{\rm d}B_z}{{\rm d}R} = {\rm i}\left(\frac{m^2}{kR^2} + k\right)B_R - \frac{Pm}{k}(\omega + mRe\,\Omega)B_R + u_R - \frac{m}{kR}X_4, \tag{2.12}$$

$$\begin{aligned}\frac{{\rm d}X_4}{{\rm d}R} &= \left(\frac{m^2}{R^2} + k^2\right)B_\phi + {\rm i}Pm(\omega + mRe\,\Omega)B_\phi \\ &\quad - 2{\rm i}\frac{m}{R^2}B_R - {\rm i}ku_\phi + 2Pm\,Re\frac{b}{R^2}B_R,\end{aligned} \tag{2.13}$$

https://doi.org/10.1017/S0022377823001356 Published online by Cambridge University Press

where X_1 is given by

$$X_1 = \frac{\mathrm{d}u_R}{\mathrm{d}R} + \frac{u_R}{R} - P - Ha^2 B_z \tag{2.14}$$

with P as the pressure fluctuation.

Here the dimensionless Reynolds number Re and the Hartmann number Ha are defined as

$$Re = \frac{R_0^2 \Omega_{\mathrm{in}}}{\nu}, \quad Ha = \frac{R_0 B_0}{\sqrt{\mu_0 \rho \nu \eta}}. \tag{2.15a,b}$$

For given Hartmann number and magnetic Prandtl number we shall compute with a linear theory the critical Reynolds number of the rotation of the inner cylinder, also for various azimuthal mode numbers m. We shall see that the excitation conditions for SMRI can easily be expressed by the magnetic Reynolds number Rm and the Lundquist number S, with the definitions

$$Rm = \frac{R_0^2 \Omega_{\mathrm{in}}}{\eta}, \quad S = \frac{R_0 B_0}{\sqrt{\mu_0 \rho \eta}} \tag{2.16a,b}$$

without influence of the molecular viscosity. The ratio of both quantities forms the magnetic Mach number of rotation,

$$Mm = \frac{Rm}{S}, \tag{2.17}$$

which describes the strength of the rotation normalized with the applied magnetic field. The majority of cosmic objects are characterized by magnetic Mach numbers larger than unity (except the magnetars). We shall discuss the relationship of the magnetic Mach number on the normalized gap width between the cylinders only for the characteristic constellation where the Reynolds number is minimal for the excitation of the instability.

The actual calculations were specifically carried out for the small magnetic Prandtl number $Pm = 10^{-5}$, but the obtained results for Rm and S are also correct for even smaller Pm (Rüdiger & Shalybkov 2002). The reason is that for small Pm the critical Reynolds number varies with $1/Pm$ so that the magnetic Reynolds number $Rm \simeq$ const. It is clear, therefore, that for $Pm = 0$ the magnetorotational instability does not exist.

3. Boundary conditions

For the solution of the differential equations of 10th order a set of 10 boundary conditions is needed. No-slip conditions for the velocity on the walls are always used, i.e. $u_R = u_\phi = \mathrm{d}u_R/\mathrm{d}R = 0$. The magnetic boundary conditions depend on the electrical properties of the walls. For perfectly conducting walls the tangential currents and the radial component of the magnetic field vanish, hence $\mathrm{d}B_\phi/\mathrm{d}R + B_\phi/R = B_R = 0$. These boundary conditions hold for both $R = R_{\mathrm{in}}$ and $R = R_{\mathrm{out}}$.

For insulating walls the magnetic boundary conditions are different at R_{in} and R_{out}, i.e. for R_{in}

$$B_R + \mathrm{i}\frac{B_z}{I_m(kR)}\left(\frac{m}{kR} I_m(kR) + I_{m+1}(kR)\right) = 0, \tag{3.1}$$

and for $R = R_{\mathrm{out}}$

$$B_R + \mathrm{i}\frac{B_z}{K_m(kR)}\left(\frac{m}{kR} K_m(kR) - K_{m+1}(kR)\right) = 0, \tag{3.2}$$

https://doi.org/10.1017/S0022377823001356 Published online by Cambridge University Press

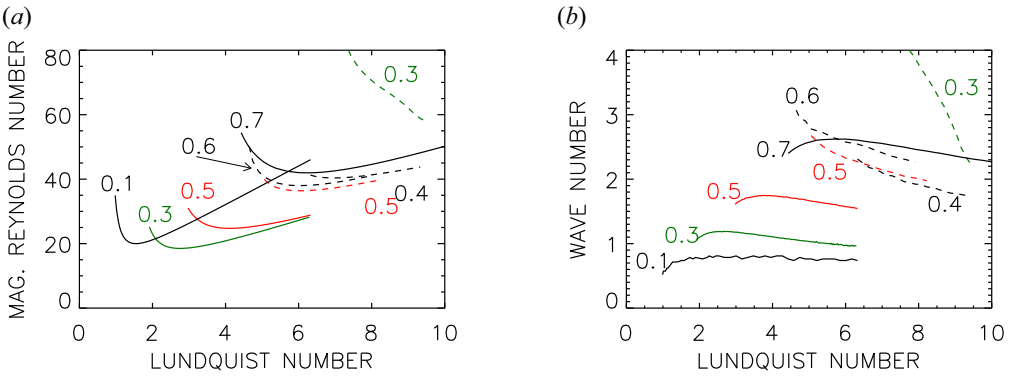

FIGURE 1. (*a*) Stability map for $m = 0$ (solid lines): $r_{\rm in} = 0.1$, $r_{\rm in} = 0.3$ (green); $r_{\rm in} = 0.5$ (red); $r_{\rm in} = 0.7$. For $m = 1$ (dashed lines): $r_{\rm in} = 0.3$ (green); $r_{\rm in} = 0.4$ $r_{\rm in} = 0.5$ (red); $r_{\rm in} = 0.6$. (*b*) The corresponding axial wavenumbers. Quasi-Keplerian differential rotation, $Pm = 10^{-5}$, perfect-conducting cylinder material.

where I_m and K_m are the modified Bessel functions. The condition for the toroidal field is $kRB_\phi = mB_z$ (Rüdiger, Schultz & Shalybkov 2003). Neutral stability of the solutions is reached for vanishing Im(ω).

The homogeneous set of (2.6)–(2.13) with the boundary conditions included determine the eigenvalue problem of the form $\mathcal{L}(k, m, Re, \omega) = 0$ for given Pm and Ha. Here $\mathcal{L}$ is a complex quantity, both its real part and its imaginary part must vanish for the critical Reynolds number. For non-axisymmetric modes the real part, Re(ω), of ω describes a drift of the pattern along the azimuth. It is the second quantity that is fixed by the complex eigenequation. For a fixed Hartmann number, a fixed Prandtl number and a given vertical wavenumber, we also find the critical Re of the system. It is minimal for a certain wavenumber defining a marginally unstable mode. The corresponding value $Re_{\rm min}$ is the minimal Reynolds number if Ha is varied and $Ha_{\rm min}$ is the Hartmann number for which the $Re_{\rm min}$ occurs. For oscillatory axisymmetric and drifting non-axisymmetric modes the real part of the frequency ω is the second eigenvalue fixed by the eigenequation.

4. General results

For perfect-conducting boundary conditions the resulting curves of marginal stability are given in figure 1 and for vacuum boundary conditions in figure 2. Figures 1(*a*) and 2(*a*) present the magnetic Reynolds numbers (minimized with the wavenumber) and figures 1(*b*) and 2(*b*) give the resulting wavenumbers, in both cases as functions of the Lundquist number. The dashed lines belong to the azimuthally drifting non-axisymmetric modes with $|m| = 1$. Generally, the latter require higher values $Rm_{\rm min}$ than the axisymmetric modes. The curves for $m = 0$ exhibit their typical shape: they are rather steep for $S < S_{\rm min}$ but they are much flatter for $S > S_{\rm min}$, where $S_{\rm min}$ is taken at the minimum of the function $Rm = Rm(S)$. For $S = O(1)$ the influence of the microscopic diffusion stops the existence of SMRI, while for much larger S it is damped by too strong external magnetic fields.

The curves of marginal stability for the axisymmetric modes only possess a lower limit of the critical Reynolds number above which the flow becomes unstable. In opposition the curves for the non-axisymmetric modes always possess a lower and an upper limit of the critical Reynolds numbers. Non-axisymmetric magnetic modes are generally stabilized by too fast shearing flow (Rädler 1986; Rüdiger *et al.* 2018*a*).

https://doi.org/10.1017/S0022377823001356 Published online by Cambridge University Press

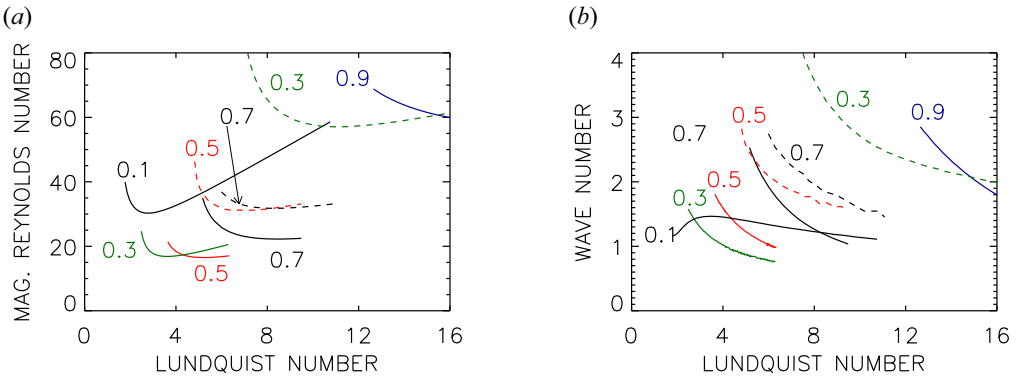

FIGURE 2. The lines of neutral stability for containers with insulating cylinders. (*a*) Stability map for $m = 0$ (solid lines) with $r_{in} = 0.1$, $r_{in} = 0.3$ (green); $r_{in} = 0.5$ (red); $r_{in} = 0.7$, $r_{in} = 0.9$ (blue); and for $m = 1$ (dashed lines) with $r_{in} = 0.3$ (green); $r_{in} = 0.5$ (red); $r_{in} = 0.7$. (*b*) The corresponding axial wavenumbers. Quasi-Keplerian differential rotation, $Pm = 10^{-5}$.

r_{in}	μ	Rm_{min}	S_{min}	k	ζ	Mm	r_{in}	μ	Rm_{min}	S_{min}	k	ζ	Mm
0.1	0.031	20.0	1.58	0.7	1.4	12.7	0.1	0.031	30.3	2.78	1.4	0.7	10.9
0.2	0.089	17.8	2.05	1.0	1.6	8.81	0.2	0.089	20.8	3.04	1.1	1.4	6.84
0.3	0.16	18.5	2.76	1.2	1.7	6.93	0.3	0.16	16.9	3.62	1.1	1.9	4.67
0.4	0.25	20.8	3.38	1.4	1.8	6.15	0.4	0.25	16.0	4.82	1.1	2.3	3.32
0.5	0.35	24.7	4.11	1.7	1.8	6.00	0.5	0.35	16.5	5.21	1.2	2.6	3.17
0.6	0.46	31.1	5.00	2.1	1.8	6.22	0.6	0.46	18.3	6.47	1.2	3.2	2.83
0.7	0.59	42.0	6.32	2.6	1.8	6.64	0.7	0.59	22.3	8.54	1.2	4.0	2.61
0.8	0.72	64.1	8.22	3.4	1.8	7.79	0.8	0.72	30.7	12.0	1.2	5.2	2.55
0.9	0.85	131	12.6	5.1	1.8	10.4	0.9	0.85	56.6	22.1	1.0	9.4	2.56
0.95	0.93	265	17.6	7.3	1.9	15.0	0.95	0.93	109	39.8	0.92	14.9	2.74

TABLE 1. The coordinates of the minima of the profiles in figures 1(*a*) and 2(*a*) for several radii the inner cylinder for different boundary conditions (left, perfect conduction; right, vacuum); $m = 0$, $Pm = 10^{-5}$. All models for quasi-Keplerian rotation laws.

4.1. *Medium gaps*

The minimum Rm_{min} in figure 1 for medium gap widths approximately behave according to $(1 - r_{in})Rm_{min} \simeq 13$ (see table 1). This relation implies that the minimal rotation rates of the inner cylinder for the considered gaps behave like $\Omega_{in} \propto 1/(1 - r_{in})$, i.e. in containers with wider gaps the instability is easier to excite. For very wide gaps, however, both the magnetic Reynolds number as well as the needed rotation rate of the inner cylinder grow to very large values. Minimal rotation rates are only possible for experiments with medium r_{in}.

In table 1 the resulting numbers Rm_{min} and S_{min} have been collected for the minima of the curves in figures 1 and 2 which we shall call the critical values. Obviously, the influences of the boundary conditions are only small for the containers with large gaps. One finds the Rm_{min} with vacuum boundary condition as always smaller than for perfect-conductor conditions (except for very thin gaps) but the S_{min} are always larger. Consequently, the corresponding magnetic Mach numbers are much larger for cylinders

https://doi.org/10.1017/S0022377823001356 Published online by Cambridge University Press

made from perfect conductors. For such containers the axial wavenumbers are always larger than for insulating walls.

With our normalizations the vertical extent δz of one cell of the instability pattern, normalized by the gap width $D = R_{\rm out} - R_{\rm in}$ between the cylinders, is given by

$$\zeta = \frac{\delta z}{D} = \frac{\pi}{k}\sqrt{\frac{r_{\rm in}}{1-r_{\rm in}}}. \tag{4.1}$$

Flat cells are described by $\zeta < 1$ while axially elongated cells possess $\zeta > 1$. For $r_{\rm in} = 0.5$ it is simply $\zeta = \pi/k$ so that for $k \simeq \pi$ the shape of the cell in the $(R–z)$ plane is almost circular. The examples given in table 1, however, show that the wavenumbers do not reach the value of π for medium $r_{\rm in}$ hence the cells are always elongated in the axial direction. This is true for models with both sorts of boundary conditions. For perfect-conducting cylinder walls $\zeta > 1$ hardly varies with $r_{\rm in}$ – the cells are always oblong. Evidently, such cells are not suitable to provide the angular momentum transport in accretion disks or galaxies.

For perfect-conducting cylinders it follows that $\zeta \simeq 1.8$ for almost all $r_{\rm in}$, while it can become significantly larger for insulating material. The minimum axial extent of a container-probing MRI pattern is thus $H \simeq 1.8D$. The aspect ratio H/D of the Princeton experiment is 2.1. It happens that the numerical ζ-values differ by almost a factor of two for models with the same geometry but with different boundary conditions.

4.2. *Extremal gaps, thin-shell approximation*

We note that for very wide gaps with $r_{\rm in} \simeq 0.1$ the characteristic Lundquist numbers $S_{\rm min}$ – for which the associated Reynolds number is minimal – are reduced to values of order unity while for very narrow gaps with $r_{\rm in} \simeq 0.95$ the Lundquist numbers are maximal. In both limits the Reynolds numbers $Rm_{\rm min}$ possess enlarged values. As also the linear dimension R_0 becomes small for small and/or large $r_{\rm in}$ the necessary inner rotation rates become very large excluding the applicability of containers with very wide and/or very narrow gaps between the cylinders for experiments. One finds that containers with $0.3 \lesssim r_{\rm in} \lesssim 0.6$ require the least rotation rates for excitation of standard magnetorotational instability. On the other hand, for both sorts of boundary conditions the models with $r_{\rm in} \simeq 0.2$ require the weakest magnetic fields.

Table 1 also gives the results for very thin gaps between the cylinders up to $r_{\rm in} = 0.95$ (Donnelly & Ozima 1960, 1962). The most striking difference due to the choice of the boundary conditions is here the numerical value of the calculated magnetic Mach number (last column). For $r_{\rm in} \to 1$ the characteristic Reynolds number grows to larger and larger values. We did not find a maximum of $Rm_{\rm min}$ for $r_{\rm in} \to 1$. As the R_0^2 runs with $1 - r_{\rm in}$ for $r_{\rm in} \to 1$ we find $\Omega_{\rm in} \to \infty$ in this limit. It should thus not be possible to work with a thin-shell approximation (Edmonds 1958) for numerical or experimental realizations of the standard MRI in TC flows.

5. The non-axisymmetric modes

The excitation of non-axisymmetric modes requires faster rotation and stronger magnetic fields than the excitation of the axisymmetric modes (figures 1 and 2; dashed lines). For medium $r_{\rm in}$ of approximately 0.5 (red) the lines of marginal stability hardly depend on the radius of the inner cylinder. As also the geometric radius R_0 is almost constant for different $r_{\rm in}$ the rotation frequencies and magnetic field amplitudes needed to excite non-axisymmetric modes are almost the same for such values of $r_{\rm in}$. However, for wide gaps and for weak magnetic fields with $S < S_{\rm min}$ the Reynolds numbers for excitation

https://doi.org/10.1017/S0022377823001356 Published online by Cambridge University Press

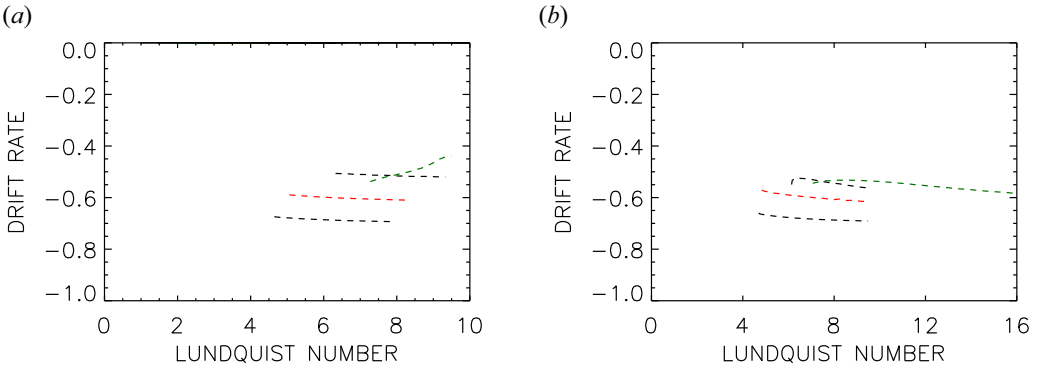

FIGURE 3. Drift rates $\omega_{dr} = \mathrm{Re}(\omega)/\Omega_{in}$ of the non-axisymmetric modes $m = 1$ (dashed lines): $r_{in} = 0.3$ (green); $r_{in} = 0.4$, $r_{in} = 0.5$ (red); $r_{in} = 0.6$. (*a*) Perfect-conducting cylinder material; (*b*) insulating cylinder material. Quasi-Keplerian differential rotation, $Pm = 10^{-5}$.

of the $m = 1$ modes are much higher than those for the excitation of the axisymmetric modes with $m = 0$. We note that the curves for the weak-field branch with $S < S_{min}$ become very steep so that the excitation of non-axisymmetric modes requires very rapid rotation.

For wide gaps between the cylinders ($r_{in} = 0.3$, green) one finds that the lowest Reynolds number belongs to much higher Lundquist numbers than for $r_{in} \simeq 0.5$. In addition, the curves for low Lundquist numbers are much steeper than the curve for the corresponding axisymmetric mode. Hence, for wide gaps with $r_{in} \lesssim 0.4$ it is almost impossible to excite the axisymmetric and the non-axisymmetric mode simultaneously by SMRI-experiments with Lundquist numbers not much higher than unity.

The non-axisymmetric modes are drifting in the azimuthal direction. The drift rates, $\omega_{dr} = \mathrm{Re}(\omega)/\Omega_{in}$, are given in figure 3. According to the relation

$$\frac{\partial\phi/\partial t}{\Omega_{in}} = -\frac{\omega_{dr}}{m}, \tag{5.1}$$

the negative ω_{dr} plotted in the figures indicate a migration of the patterns in the direction of the global rotation – for both sorts of boundary conditions. In all cases the azimuthal migration is faster than the rotation of the outer cylinder ($\omega_{dr} > \mu$).

6. Marginal stability for weak fields

It is possible to apply weak magnetic fields with $S < S_{min}$. Then, however, the Reynolds numbers necessary for excitation basically grow and the unstable wavenumbers become smaller, i.e. the cells become longer. Figure 4 demonstrates these weak-field solutions with $S < S_{min}$ for $r_{in} = 0.3$ (figure 4*a*) and $r_{in} = 0.4$ (figure 4*b*). The vertical lines represent the magnetic fields $B = 2150\,\mathrm{G}$ (corresponding to $S = 0.96$) and $B = 2750\,\mathrm{G}$ (corresponding to $S = 1.22$) reported for gallium SMRI experiments by Wang *et al.* (2022*b*). We have also to note the influence of the boundary conditions: for insulating cylinders the curves for weak fields with $S < S_{min}$ are so steep that the necessary critical Reynolds numbers at the vertical lines exceed the Rm_{min} of the curves by more than one order of magnitude. This extreme enhancement is slightly reduced for perfect-conducting cylinder material but still the enhancement of the critical Reynolds number is by a factor of three relative to Rm_{min}. This is even a minimum value as the real cylinders are, by far, not perfect-conducting. For

https://doi.org/10.1017/S0022377823001356 Published online by Cambridge University Press

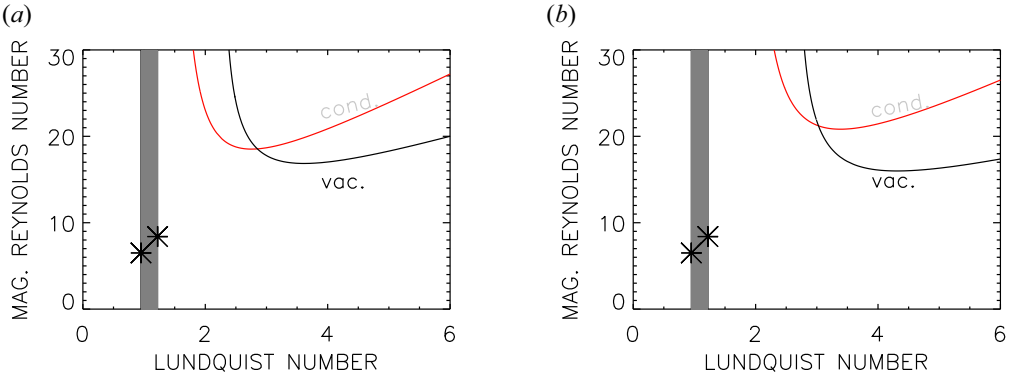

FIGURE 4. Stability lines of the axisymmetric modes for $r_{\rm in} = 0.3$ (a) and $r_{\rm in} = 0.4$ (b) of containers with perfect-conducting cylinders (red) and with insulating cylinders (black). The lines of experiments with imperfectly conducting cylinders are located between the curves marked with 'vac.' and 'cond.'. The vertical lines mark the Lundquist numbers after (2.15a,b) for the Princeton MRI-experiments represented by the lowest and the highest solid circles in their figure 2(a) (magnetic fields 2150 G and 2750 G) while the asterisks belong the used magnetic Reynolds numbers. With the planned Dresdyn sodium experiment the same magnetic field amplitudes will belong to Lundquist numbers exceeding 15.

galinstan as the fluid and stainless steel as the (outer) cylinder material the ratio

$$\hat{\sigma} = \frac{\sigma_{\rm cyl}}{\sigma_{\rm fl}} \tag{6.1}$$

of the electric conductivities of the cylinders and the fluid is 0.47, which neither well approaches perfect-conduction nor vacuum boundary conditions. For sodium experiments one finds $\hat{\sigma} \simeq 0.16$, hence the vacuum boundary conditions might provide the appropriate description. Rüdiger *et al.* (2018b) derived the form of the boundary conditions with finite values of (6.1) and have shown that for $\hat{\sigma}$ of order unity the resulting eigenvalues can approximately be interpolated between the values for $\hat{\sigma} = 0$ (insulating boundaries) and $\hat{\sigma} = \infty$ (perfect-conducting boundaries).

Detailed consequences of the application of weak magnetic fields for the excitation of the axisymmetric mode are shown in figure 4. The Lundquist number (2.15a,b) is marked by vertical lines for a container with $R_{\rm out} = 20.3\,{\rm cm}$, $r_{\rm in} = 0.35$ filled with galinstan ($\rho = 6.4\,{\rm g\,cm^{-3}}$ and $\eta = 2428\,{\rm cm^2\,s^{-1}}$) with its magnetic Prandtl number of 1.4×10^{-6}. The numbers correspond to the gallium experiment by Wang *et al.* (2022b). The maximally possible uniform magnetic field in this experiment given as 4800 G corresponds to a Lundquist number after (2.15a,b) of $S = 2.1$. One finds with figure 4 that for such fields the minimum magnetic Reynolds number for marginal stability must exceed 20, corresponding to a minimum value of 10.8 in the notation of Wang *et al.* (2022b). The left vertical lines in figure 4 represent the reported MRI realization for Lehnert number $B_0 = 0.2$[1] and Reynolds number 3.4 (their notation, lower asterisk) provided by their figure 2(a). The experiment with the fastest rotation (upper asterisk) belongs to a Lundquist number of $S = 1.22$ (right vertical lines).

If the typical parameters of the experiment with almost Keplerian flow and with maximal Reynolds number are transformed to our definitions (2.15a,b), one obtains

[1] not to be confused with the applied magnetic field B_0 in the notations (2.15a,b) and (2.16a,b).

https://doi.org/10.1017/S0022377823001356 Published online by Cambridge University Press

maximal Reynolds numbers of $Rm = 8.4$ (right asterisks in the plots) which does not reach the values required for marginal instability at any Lundquist number. This deficit is particularly drastic for vacuum boundary conditions.

Because of the exceptional meaning of the Kepler rotation in astrophysics, all calculations have been performed for the rotation law with $q = 1.5$. The question may arise how relevant the results are for experiments with rotation laws somewhat steeper than the Keplerian one. The coefficient q in the Princeton experiment is $q = 1.59$. As mentioned above, the same pair of qs yields $\mu = 0.35$ and $\mu = 0.33$ for $r_{\rm in} = 0.5$. For this case table 1 provides a magnetic Reynolds number of 24.7 for perfect-conducting boundaries. This is 14 % higher than the value 21.3 given in the Introduction for $\mu = 0.33$, representing the difference of the Reynolds numbers for Keplerian rotation with $q = 1.5$ and for slightly super-Keplerian rotation with $q = 1.59$. For the latter one has thus to shift the curves in figure 4 downwards by (say) 14 %. The uncertainties due to the application of the too ideal boundary conditions, however, will overcompensate this small shift so that the stability line of the real experiment will certainly remain in the area between the limiting curves in figure 4.

Our results comply with the finding of Goodman & Ji (2002) in their figures 1 and 2, that containers with insulating walls of $r_{\rm in} = 0.33$ including a quasi-Keplerian flow do not allow the excitation of SMRI with an applied field of less than 2750 G. Even with perfect-conducting cylinders the curves are so steep for $S < S_{\rm min}$ that the needed rotation rates of the cylinders are too high.

7. Flat cells

As demonstrated by table 1 the cell structure for the axisymmetric modes is nearly circular in the $(R - z)$-plane for wide gaps and rather elongated in the axial direction for narrow gaps. It is thus still unclear whether the standard MRI is also able to produce flat cells with $\zeta \ll 1$ which are necessary to appear in experiments with a flat container ($H < D$) and/or in flat cosmical objects such as accretion disks and galaxies. For the latter, the magnetic Mach number of rotation does not exceed values of 10, as it is the case for the solutions given in table 1.

We have therefore to probe whether eigensolutions exist for finite Rm and S when, for example, $\zeta = 0.1$ is required. From (4.1) one obtains for (say) $r_{\rm in} = 0.1$ that solutions with $k = 10.5$ are matched for $\zeta = 0.1$.

Figure 5 shows the results. Indeed, the envisaged flat cells exist in the axially unbounded container and even for similar Lundquist numbers as for the solutions with the lowest Reynolds numbers and the elongated cells. The actual magnetic Reynolds numbers for flat cell structures, however, are much higher than before. Hence, the magnetic Mach numbers for flat cells are also higher than for the elongated cells summarized in table 1. They are larger than 10 and grow for growing flatness. This result complies with that of a global model of a flat galaxy for magnetic Prandtl number $Pm \geq 1$ (Kitchatinov & Rüdiger 2004). The flatter the cells, the stronger the dissipation and the harder the differential rotation must work to excite the instability while the magnetic field needed for the rotation minimum remains unchanged. We also learn from figure 5 that the influence of the actual boundary condition is remarkably weak.

8. Discussion

The influence of the position $r_{\rm in}$ of the inner cylinder of TC flows on the excitation of the magnetorotational instability has been studied. To demonstrate the results we shall switch

https://doi.org/10.1017/S0022377823001356 Published online by Cambridge University Press

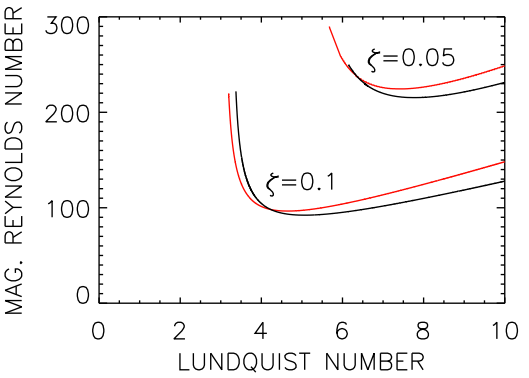

FIGURE 5. Lines of marginal stability for $r_{\rm in} = 0.1$ and a fixed axial wavenumber of $k = 10.5$ for $\zeta = 0.1$ and $k = 21$ for $\zeta = 0.05$: perfect-conductingcylinders (red); insulating cylinders (black). The flatter the cell the higher the magnetic Mach number. The influence of the boundary conditions is rather weak; $m = 0$, quasi-Keplerian rotation, $Pm = 10^{-5}$.

to the more traditional representations

$$Rm^* = \frac{R_{\rm out}^2 \Omega_{\rm in}}{\eta}, \quad S^* = \frac{R_{\rm out} B_0}{\sqrt{\mu_0 \rho \eta}}, \tag{8.1a,b}$$

(where simply the $r_{\rm in}$-dependent R_0 in the parameters (2.15*a*,*b*) has been replaced by the fixed $R_{\rm out}$) which for given outer cylinder size $R_{\rm out}$ form minimal normalized inner rotation rates and magnetic field amplitudes needed for excitation of the instability. These quantities are plotted as function of $r_{\rm in}$ in figure 6 for both sorts of boundary conditions. The main result is that too narrow or too wide gaps would require very high rotation rates or very strong magnetic fields. For $0.3 \lesssim r_{\rm in} \lesssim 0.6$ the dependence of the numbers on $r_{\rm in}$ is rather weak. The minima for conducting cylinders are at $r_{\rm in} \simeq 0.4$ for the rotation rate and at $r_{\rm in} \simeq 0.2$ for the magnetic field. We also note that the influence of the boundary conditions is opposite for rotation and field. For vacuum conditions the needed rotation rates are mostly lower than for perfect-conduction conditions but the needed magnetic fields are higher for insulating cylinders.

One may ask whether for given outer radius not only the inner rotation frequency has a minimum for a certain $r_{\rm in}$ but also the momentum to maintain this critical $\Omega_{\rm in}$. To this end one has to multiply Rm^* from figure 6(*a*) with $r_{\rm in}^2$. The result is a monotonously increasing function for $r_{\rm in} \geq 0.1$. In this range there is no minimum at any $r_{\rm in}$ for the power to drive the inner cylinder. Such a minimum could maximally exist very close to the axis which, however, is not relevant for real constructions.

The experiment with the fastest rotation ($Rm = 4.5$) by Wang *et al.* (2022*b*) corresponds to $Rm^* = 37$ which is certainly below the curves in figure 6(*a*). A similar situation holds with respect to the magnetic field: the given maximal possible field of 4800 G provides a Lundquist number of $S^* = 4.4$ which again does not reach the minimum value in figure 6(*b*). Compared with our calculations the reported experiments are clearly subcritical with respect to the magnetic field and the reported rotation rates. There is no value of $r_{\rm in}$ for which the applied rotation rates and/or magnetic fields are supercritical by a large margin. If TC experiments which are subcritical in the described sense provide unstable modes then extra influences (such as electric currents, non-zonal flows or non-axial field components) besides homogeneous axial magnetic background fields and differential rotation as the standard combination of SMRI should be active.

https://doi.org/10.1017/S0022377823001356 Published online by Cambridge University Press

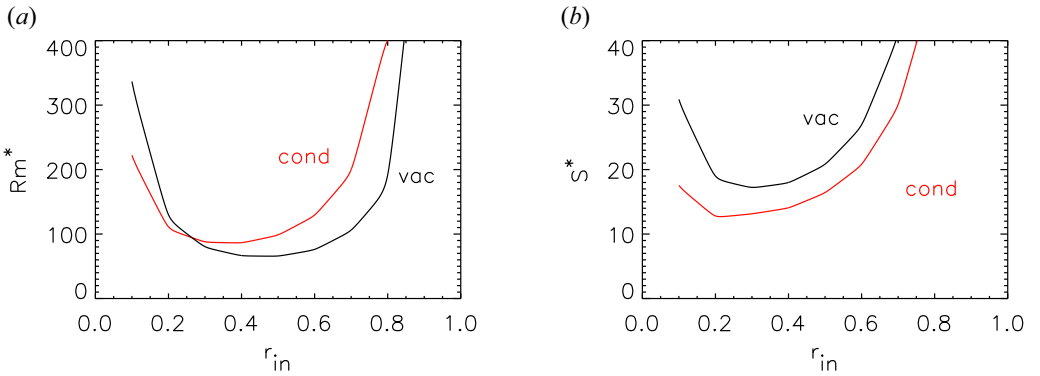

FIGURE 6. The magnetic Reynolds number (*a*) and the Lundquist number (*b*) after the definitions (8.1*a*,*b*) representing the normalized inner rotation rate and the magnetic field amplitude needed for excitation versus $r_{\rm in}$. Quasi-Keplerian differential rotation, $Pm = 10^{-5}$, perfect-conducting cylinder material (red), insulating cylinders (black). The numbers are taken from table 1.

Nonlinear simulations of axially unbounded SMRI models with medium magnetic Prandtl numbers never did provide instability patterns if for given Lundquist number the applied Reynolds number is lower than the minimum Reynolds number taken from the linear theory (Rüdiger *et al.* 2018*a*). For an interpretation of the observed axisymmetric and even non-axisymmetric instabilities (see Wang *et al.* 2022*a*) the specific role of the Ekman–Hartmann layers inside the copper lids indeed leading to subcritical instability excitations should be discussed (Gilman & Benton 1968; Szklarski & Rüdiger 2007; Gissinger, Goodman & Ji 2012) but this is not the task of this paper.

Acknowledgements

F. Stefani (Dresden-Rossendorf) is acknowledged for discussions of the presented problem and a critical reading of the manuscript. This research received no specific grant from any funding agency, commercial or not-for-profit sectors. The authors report no conflict of interest.

Editor S. Tobias thanks the referees for their advice in evaluating this article.

Declaration of interests

The authors report no conflict of interest.

REFERENCES

DONNELLY, R.J. & OZIMA, M. 1960 Hydromagnetic stability of flow between rotating cylinders. *Phys. Rev. Lett.* **4**, 497–498.

DONNELLY, R.J. & OZIMA, M. 1962 Experiments on the stability of flow between rotating cylinders in the presence of a magnetic field. *Proc. R. Soc. Lond.* A **266**, 272–286.

EDMONDS, F.N. JR. 1958 Hydromagnetic stability of a conducting fluid in a circular magnetic field. *Phys. Fluids* **1**, 30–41.

GILMAN, P.A. & BENTON, E.R. 1968 Influence of an axial magnetic field on the steady linear Ekman boundary layer. *Phys. Fluids* **11** (11), 2397–2401.

GISSINGER, C., GOODMAN, J. & JI, H. 2012 The role of boundaries in the magnetorotational instability. *Phys. Fluids* **24** (7), 074109–074109–15.

https://doi.org/10.1017/S0022377823001356 Published online by Cambridge University Press

GOODMAN, J. & JI, H. 2002 Magnetorotational instability of dissipative Couette flow. *J. Fluid Mech*. **462**, 365–382.

HOLLERBACH, R. & RÜDIGER, G. 2005 New type of magnetorotational instability in cylindrical Taylor-Couette flow. *Phys. Rev. Lett*. **95** (12), 124501.

HOLLERBACH, R., TEELUCK, V. & RÜDIGER, G. 2010 Nonaxisymmetric magnetorotational instabilities in cylindrical Taylor-Couette flow. *Phys. Rev. Lett*. **104** (4), 044502.

JI, H., GOODMAN, J. & KAGEYAMA, A. 2001 Magnetorotational instability in a rotating liquid metal annulus. *Mon. Not. R. Astron. Soc*. **325**, L1–L5.

KITCHATINOV, L.L. & RÜDIGER, G. 2004 Seed fields for galactic dynamos by the magnetorotational instability. *Astron. Astrophys*. **424**, 565–570.

OGILVIE, G.I. & PRINGLE, J.E. 1996 The non-axisymmetric instability of a cylindrical shear flow containing an azimuthal magnetic field. *Mon. Not. R. Astron. Soc*. **279**, 152–164.

RÄDLER, K.H. 1986 Effect of differential rotation on magnetic fields of cosmical bodies. In *Plasma Astrophysics* (ed. T. Duc Guyenne & L.M. Zeleny), ESA Special Publication, vol. 251, p. 569.

RÜDIGER, G., GELLERT, M., HOLLERBACH, R., SCHULTZ, M. & STEFANI, F. 2018*a* Stability and instability of hydromagnetic Taylor-Couette flows. *Phys. Rep*. **741**, 1–89.

RÜDIGER, G., HOLLERBACH, R., STEFANI, F., GUNDRUM, T., GERBETH, G. & ROSNER, R. 2006 The traveling-wave MRI in cylindrical Taylor-Couette flow: comparing wavelengths and speeds in theory and experiment. *Astrophys. J*. **649**, L145–L147.

RÜDIGER, G., SCHULTZ, M. & SHALYBKOV, D. 2003 Linear magnetohydrodynamic Taylor-Couette instability for liquid sodium. *Phys. Rev.* E **67** (4), 046312.

RÜDIGER, G., SCHULTZ, M., STEFANI, F. & HOLLERBACH, R. 2018*b* Magnetorotational instability in Taylor-Couette flows between cylinders with finite electrical conductivity. *Geophys. Astrophys. Fluid Dyn*. **112** (4), 301–320.

RÜDIGER, G. & SHALYBKOV, D. 2002 Stability of axisymmetric Taylor-Couette flow in hydromagnetics. *Phys. Rev.* E **66** (1), 016307.

RÜDIGER, G. & ZHANG, Y. 2001 MHD instability in differentially-rotating cylindric flows. *Astron. Astrophys*. **378**, 302–308.

SCHARTMAN, E., JI, H. & BURIN, M.J. 2009 Development of a Couette-Taylor flow device with active minimization of secondary circulation. *Rev. Sci. Instrum*. **80** (2), 024501.

SCHARTMAN, E., JI, H., BURIN, M.J. & GOODMAN, J. 2012 Stability of quasi-Keplerian shear flow in a laboratory experiment. *Astron. Astrophys*. **543**, A94.

SEILMAYER, M., GALINDO, V., GERBETH, G., GUNDRUM, T., STEFANI, F., GELLERT, M., RÜDIGER, G., SCHULTZ, M. & HOLLERBACH, R. 2014 Experimental evidence for nonaxisymmetric magnetorotational instability in a rotating liquid metal exposed to an azimuthal magnetic field. *Phys. Rev. Lett*. **113** (2), 024505.

STEFANI, F., GUNDRUM, T., GERBETH, G., RÜDIGER, G., SCHULTZ, M., SZKLARSKI, J. & HOLLERBACH, R. 2006 Experimental evidence for magnetorotational instability in a Taylor-Couette flow under the influence of a helical magnetic field. *Phys. Rev. Lett*. **97** (18), 184502.

SZKLARSKI, J. & RÜDIGER, G. 2007 Ekman-Hartmann layer in a magnetohydrodynamic Taylor-Couette flow. *Phys. Rev.* E **76** (6), 066308.

VELIKHOV, E. 1959 Stability of an ideally conducting liquid flowing between cylinders rotating in a magnetic field. *Sov. Phys. JETP* **36**, 1389–1404.

WANG, Y., GILSON, E.P., EBRAHIMI, F., GOODMAN, J., CASPARY, K.J., WINARTO, H.W. & JI, H. 2022*a* Identification of a non-axisymmetric mode in laboratory experiments searching for standard magnetorotational instability. *Nat. Commun*. **13**, 4679.

WANG, Y., GILSON, E.P., EBRAHIMI, F., GOODMAN, J. & JI, H. 2022*b* Observation of axisymmetric standard magnetorotational instability in the laboratory. *Phys. Rev. Lett*. **129** (11), 115001.